NANO LETTERS

2008
Vol. 8, No. 10
3146-3150

The Impact of Nanocontact on Nanowire Based Nanoelectronics

Yen-Fu Lin and Wen-Bin Jian*

Department of Electrophysics, National Chiao Tung University, Hsinchu 30010, Taiwan

Received May 10, 2008; Revised Manuscript Received August 3, 2008

ABSTRACT

Nanowire-based nanoelectronic devices will be innovative electronic building blocks from bottom up. The reduced nanocontact area of nanowire devices magnifies the contribution of contact electrical properties. Although a lot of two-contact-based ZnO nanoelectronics have been demonstrated, the electrical properties bringing either from the nanocontacts or from the nanowires have not been considered yet. High quality ZnO nanowires with a small deviation and an average diameter of 38 nm were synthesized to fabricate more than thirty nanowire devices. According to temperature behaviors of current−voltage curves and resistances, the devices could be grouped into three types. Type I devices expose thermally activated transport in ZnO nanowires and they could be considered as two Ohmic nanocontacts of the Ti electrode contacting directly on the nanowire. For those nanowire devices having a high resistance at room temperatures, they can be fitted accurately with the thermionic-emission theory and classified into type II and III devices according to their rectifying and symmetrical current−voltage behaviors. The type II device has only one deteriorated nanocontact and the other one Ohmic contact on single ZnO nanowire. An insulating oxide layer with thickness less than 20 nm should be introduced to describe electron hopping in the nanocontacts, so as to signalize one- and high-dimensional hopping conduction in type II and III devices.

Quasi-one-dimensional (Q1D) nanostructures of carbon nanotubes,[1] silicon,[2,3] and metal oxide[4] nanowires (NWs), nanorods, and nanobelts[5] have been synthesized in the past decade. One of the novel concepts for the emerging field of nanotechnology is the low cost synthesis method to create a large quantity of nanomaterials.[6] An another beneficial concept might be making electronic devices such as diodes and transistors by using the bottom-up assembling process[7] rather than the high technical top-down engraving manner. A preliminary field-effect transistor (FET) by using the Q1D carbon nanotubes has immediately been demonstrated,[8] and as a consequence it demands the early preparative studies and probing of electrical transport in individual Q1D nanostructures.[9] To fit the requirements and to accomplish the goals as mentioned above, the contact problem, which plays the most important role in the Q1D nanostructure devices, must be overcome.

ZnO has attracted intense attention due to its large exciton binding energy for the room-temperature (RT) lasing as well as photoconductive applications, being heavily doped to form transparent conductors, and piezoelectric power generators.[10] In particular, since metal oxides such as ZnO are physically and chemically more stable than Ge, Si, and other semiconductors at RT, ZnO-based nanostructures could be a better candidate for nanoelectronics. In fact, ZnO NWs were used to construct two- and four-contact (or four-terminal) nanoelectronic devices for ultraviolet photodetectors,[11] gas sensors,[12,13] FETs,[13−15] Schottky diodes,[16,17] logic circuits,[18] and light-emitting diodes.[19] Current−voltage ($I-V$) characteristics of ZnO NW devices were obtained to reveal either a Schottky type feature, which manifests itself as a rectifying and upward bending $I-V$ curve in forward bias voltage,[16] or a symmetrically downward bending $I-V$ curve.[14] In order to separate contact from the intrinsic resistance of the NWs, Zhang et al.[20] proposed the field-effect based model to analyze experimental $I-V$ curves from two-contact measurements. On the other hand, electron transport in ZnO NW devices exposed either the thermally activated transport[14] or variable-range-hopping (VRH) conduction.[21]

The importance of contact effects on NW nanoelectronics has been adverted earlier.[22] Bachtold et al.,[23] for example, adopted e-beam irradiation to build low-ohmic contact on carbon nanotubes and Stern et al.[24] recognized that the specific contact resistivity was strongly dependent on the intrinsic GaN NW resistivity. Additionally, we previously deduced from experiments that intrinsic NW resistance could be estimated by using NW devices with a low RT resistance.[25] In this work, thirty more two-contact NW devices were fabricated to explore the $I-V$ characteristics and electron transport in either the nanocontacts or the NWs. The electrical transport properties are discussed in accordance with the solid state and semiconductor physics theories to explore the nanocontact property.

* To whom correspondence should be addressed. E-mail: wbjian@mail.nctu.edu.tw.

10.1021/nl801347x CCC: $40.75
Published on Web 08/27/2008

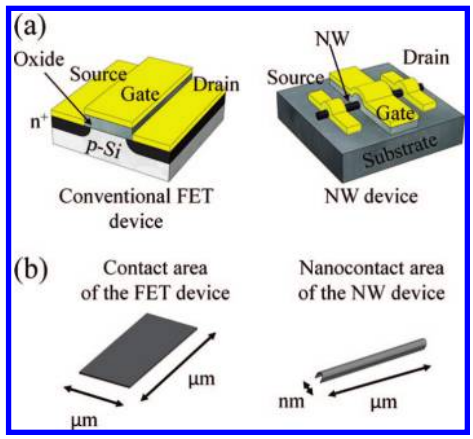

Figure 1. (a) Schematic diagrams of conventional FET and NW devices with their corresponding contact areas (b) illustrated.

Cylindrical ZnO NWs with precisely controlled diameters of 38 ± 4.6 nm[26] were employed to construct ZnO NW devices. Since oxide materials have a relatively high resistivity and the resistance rises with a reduction of the size and dimension, a 400 nm thick SiO_2 layer was capped on the silicon wafer to prevent from current leakages through the substrate. After the substrate was photolithographically patterned with gold micron-electrodes, a dispersion process followed to deposit as-grown ZnO NWs. A single ZnO NW was positioned and two Ti/Au (~20/100 nm in thickness) nanometer electrodes, taken as source and drain electrodes, were deposited on it in conjunction with micron electrodes by using standard e-beam lithography and thermal evaporation. The source and drain electrodes were separated at a constant distance of ~1 μm. The as-fabricated ZnO NW devices were loaded in a liquid-nitrogen cryostat for their temperature dependent $I-V$ curve measurements.

Before we start to discuss experimental results, the significance of nanocontact resistance for NW-based nanoelectronics should be considered. Figure 1a gives schematic diagrams of a conventional *n*-channel metal-oxide-semiconductor FET and a NW device. The source and drain electrodes of the conventional FET device are connected by a two-dimensional conducting channel of a surface inversion layer while those of the NW device are conjunctive through a Q1D channel of a single NW. Since the channel cross-sectional size of the NW has the same order of magnitude as the de Broglie wavelength of the electron, the ballistic quantum transport might contribute in the innovatively developed NW devices. Figure 1b illustrates the corresponding contact areas of a conventional FET and a NW device. As a general rule, the contact resistance R_C is inversely relative to the contact area A_C as[24]

$$R_C = \frac{\rho_C}{A_C} \tag{1}$$

where ρ_C is the specific contact resistivity. Remarkably, the contact and nanocontact areas showing in Figure 1b have an area difference by 2 or 3 orders of magnitude. Therefore, the nanocontact resistance R_C of the NW device could be hundred or thousand times higher than that of the conventional FET device, even though they might have the same specific contact resistivity ρ_C. Consequently, the distinctive attribute of the greatly diminished contact area in the NW device intensifies exceptionally the nanocontact resistance which dominates the electrical properties of the nanowire based nanoelectronics.

When the nanocontacts of the NW device are Ohmic type, according to solid state and semiconductor physics, electrical conductivity reveals linear $I-V$ reliance in agreement with Ohm's law as $E = J\rho$ or $V = IR$,[27] where E, J, ρ, and R are the electric field, current density, resistivity, and resistance, respectively. Moreover, its zero-voltage resistance unveils the intrinsic NW transport property of thermally activated transport, which reflects temperature T dependence of carrier concentration under the assumption of a constant mobility in a narrow temperature range, in conformity with the form[28]

$$R = R_0 \exp\left(\frac{E_A}{2kT}\right) \tag{2}$$

where E_A, k, and R_0 are the activation energy, the Boltzmann constant, and a material dependent constant, respectively. Otherwise, when the nanocontacts are Schottky type, the $I-V$ relationship predicted by the thermionic-emission theory coincides with the equation[29]

$$J = A^{**}T^2 \exp\left(-\frac{q\Phi_{BE}}{kT}\right)\exp\left(\frac{qV}{nkT}\right)\left[1 - \exp\left(-\frac{qV}{kT}\right)\right] \tag{3}$$

where A^{**}, q, Φ_{BE}, and n are the Richardson constant, charge, effective barrier, and ideality factor, respectively. Schottky type contacts result in the zero-voltage specific contact resistivity of the form

$$\rho_C = \frac{k}{A^{**}Tq}\exp\left(\frac{q\Phi_{BE}}{kT}\right) \tag{4}$$

On the other hand, the metal-semiconductor interface might have disorders or noncrystalline interfacial structures. The contact resistance enhances due to its tiny contact area so it may dominate the total resistance of the NW device. The temperature behavior of the zero-voltage resistance will show VRH conduction which complies with the equation[21,30]

$$R = R_0 \exp\left(\left(\frac{T_0}{T}\right)^{1/p}\right) \tag{5}$$

where T_0 and R_0 are constants. The exponent parameter p is 2, 3, or 4 for a one-, two-, or three-dimensional disordered system, respectively. In particular, the thermally activated transport of eq 2 can be taken as eq 5 with the exponent parameter $p = 1$. In the following paragraphs, we exercise the transport equations to analyze the temperature behavior of the $I-V$ curves and the resistance of our as-fabricated two-contact ZnO NW devices. Although the analysis in the light of macroscopic transport theories could give one way, and there might be other ways, to understand the basic mechanisms of our NW devices, we demonstrate that our data can be fitted concordantly with equations described in this paragraph.

Even though the distance between the two contacts was kept constant, we still observed different RT resistances for our ZnO NW devices. According to their RT resistances and $I-V$ curves, the devices were grouped into three different types. Figure 2a presents the first type, type I, ZnO NW

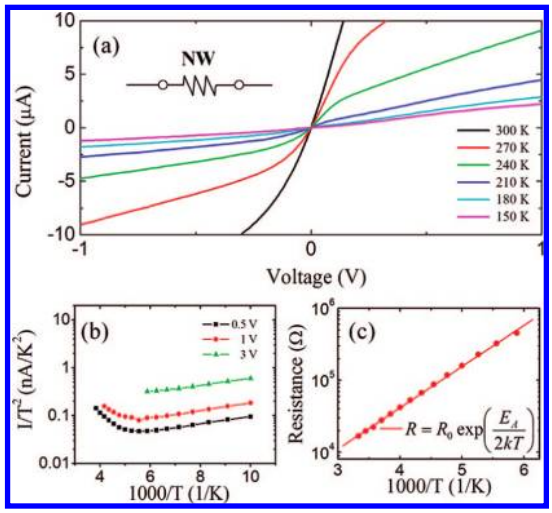

Figure 2. (a) $I-V$ curves of a type I ZnO NW device with a RT resistance of ~15 kΩ. The inset introduces a model of circuit diagram for type I devices. (b) I/T^2 as a function of inverse temperature at various bias voltages. (c) Resistance as a function of temperature revealing electron transport in the type I device.

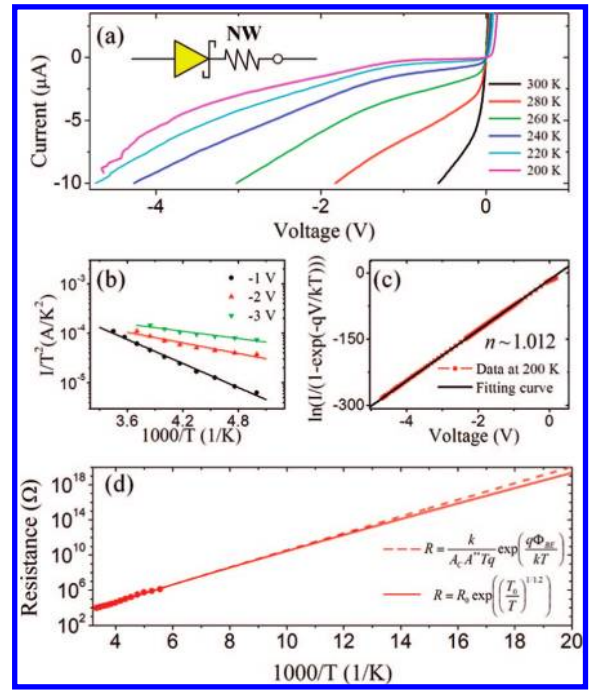

Figure 3. (a) $I-V$ curves of a type II ZnO NW device with a RT resistance of ~50 kΩ. The inset introduces a model of circuit diagram for type II devices. (b) I/T^2 as a function of inverse temperature at various bias voltages. (c) $\ln(I/(1-\exp(-qV/kT)))$ as a function of voltage. (d) Resistance as a function of temperature revealing electron transport in this type II device. The dashed and solid lines are best fittings (see text) of eqs 4 and 5, respectively.

device with characteristics of a lower RT resistance, a linear $I-V$ demeanor in low voltage range, and a symmetrically downward bending feature in $I-V$ curves. The low RT resistance and linear $I-V$ dependence imply that both of the two nanocontacts are Ohmic type. Moreover, the temperature behavior of current at various bias voltage is analyzed with regard to the thermionic-emission theory of eq 3 and shown in Figure 2b but we did not find any concordance. The result of inconsistence with Schottky contact supports the Ohmic type contacts for type I devices as well. The circuit diagram of type I devices with two Ohmic nanocontacts (indicated as circles) and one ZnO NWs (a resistance symbol) is given in the inset of Figure 2a. Since both the two nanocontacts are Ohmic type, the device resistance could mainly come from the intrinsic ZnO NW resistance. On the other hand, the zero-voltage resistances as a function of temperature are displayed in Figure 2c. The electron transport behavior can be well apprehended in agreement with the thermally activated transport (eq 2) of electrons in ZnO NWs. The intrinsic ZnO NW resistance unveils thermally activated transport of conduction through the NW which conforms to our four-terminal measurements[31] and other groups' results.[32,33] Since the conduction through the nanowire has been unambiguously investigated in type I devices, the other devices having higher RT resistances could give electrical properties at nanocontacts.

A rectifying behavior on $I-V$ curves, especially at low temperatures, has been unambiguously obtained and presented in Figure 3a. We notice that the nonsymmetrical $I-V$ curves of the type II NW device could only originate from one and only one Schottky nanocontact with the other one of Ohmic type. A circuit diagram model is offered in the inset of Figure 3a to depict the Schottky nanocontact, the ZnO NW, and the Ohmic nanocontact from left to right. The analyses in accordance with thermionic-emission theory of eq 3 are given in Figure 3b,c. For type II devices, we observed linear dependence between $\ln(I/T^2)$ and $1/T$ with a slope indicating the effective Schottky barrier in the Schottky nanocontact. At a high bias voltage, the slope tends to zero which denotes the vanishing of effective Schottky barrier Φ_{BE} when the bias approaches the break down voltage. Moreover, the $I-V$ curve in a wide voltage range introduced in Figure 3c fits precisely with eq 3 both in forward and reverse bias voltages. Intriguingly and surprisingly, the ideality factor estimated from our fitting is very close to the ideal value of 1. Alternatively, the RT resistance of type II devices ranges from near the upper bound RT resistance of type I devices to that of type III devices as will be acquainted in the next paragraphs. The temperature dependence of resistance $R(T)$ in Figure 3d indicates that the electron transport behavior cannot be solely interpreted by the thermally activated transport in ZnO NW. In addition, electron transport in the Schottky nanocontact should be taken into consideration. We found that electron transport in these type II devices departs from eq 2 and starts to reconcile with eqs 4 or 5, and we noticed that the fittings with either Schottky contact (eq 4) or VRH conduction (eq 5) do not make a significant difference at temperatures above 100 K. These results suggest that electrical properties, including $I-V$ curves and zero-voltage resistances, mostly arise from the single Schottky nanocontact in the type II NW devices.

Typical characteristics of the last type, the type III ZnO NW devices with analyses through thermionic-emission theory are given in Figure 4. First of all, the $I-V$ curves in Figure 4a reveal symmetrical and an upward bending feature,

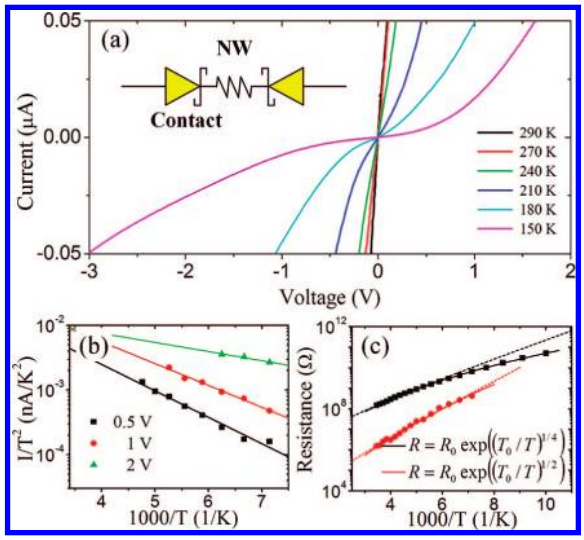

Figure 4. (a) $I-V$ curves of a type III ZnO NW device with a RT resistance of ~1.5 MΩ. The inset introduces a model of circuit diagram for type III devices. (b) I/T^2 as a function of inverse temperature at various bias voltages. (c) Resistance as a function of temperature revealing electron transport in this type III device (red circles) and in another type III device having a RT resistance of ~128 MΩ (black squares). The dashed and solid lines are best fittings (see text) of eqs 4 and 5, respectively.

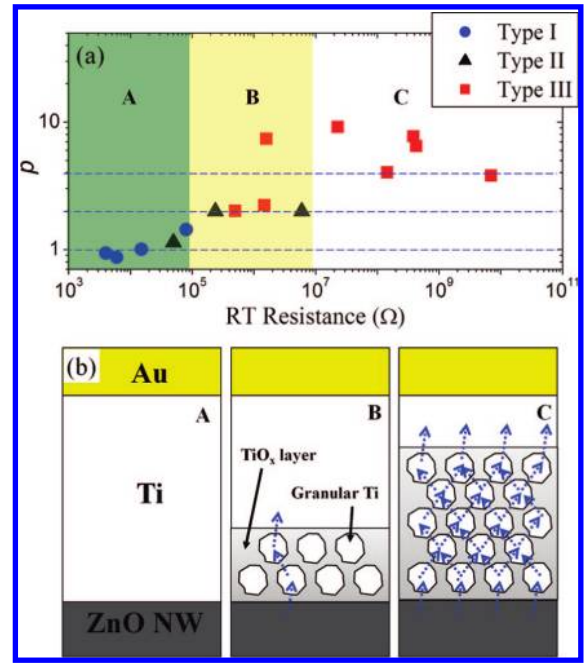

Figure 5. (a) The fitting exponent parameters p as a function of RT resistance for our as-fabricated ZnO NW devices of type I, II, and III, marked as blue circles, black triangles, and red squares, respectively. The figure is approximately separated into Regions A, B, and C according to the exponent parameters of our devices. (b) Three different nanocontact models corresponding to the ZnO NW devices belonging to Regions A, B, and C of panel a.

and the data can be fitted well with thermionic-emission theory of eq 3 in reverse bias voltage. The linear dependence of $\ln(I/T^2)$ and $1/T$ at various bias voltage appears prominently in Figure 4b that supports our idea of Schottky contacts for type III devices. Since no forward bias $I-V$ reliance of a Schottky diode is spotted and the currents in both positive and negative voltages agree well with the reverse-bias thermionic-emission theory (see Figure 4a,b), we propose a model of two back-to-back Schottky contacts, which is commonly addressed to explain nonlinear $I-V$ curves of semiconductor NW devices,[34,35] in the inset of Figure 4a to demonstrate the type III devices. As for zero-voltage resistance, we obtained several different temperature dependent behaviors. Two typical sets of resistance data are presented in Figure 4c with the best fittings of dashed and solid lines following Schottky contact (eq 4) and VRH conduction (eq 5), respectively. In this case, we found that the data points vary from the ideal Schottky contact form of eq 4 at temperatures below 200 K. Including the information of high RT resistances for type III devices as well as the best fitting in accordance with VRH conduction form of eq 5, we propose that a deteriorated contact between the Ti electrode and the ZnO NW forms due to a noncrystalline interface layer or titanium oxides. Owing to a diminished nanocontact area, a poor specific contact resistivity results in a high contact resistance and dominates electrical properties of the type III NW devices.

To discuss electron transport in ZnO NW devices and to fit their temperature dependent resistance, we adopted VRH conduction of eq 5 and included the exponent parameter p of 1 for thermally activated transport. The estimated exponent parameters as a function of device RT resistance are given in Figure 5a. An unambiguous trend of a rising exponent parameter with an increase of RT resistance has been detected that signals worsened electrical properties in the nanocontacts. Moreover, the graph can be approximately separated into Regions A, B, and C with an exponent parameter of about 1, 2, and bigger than 3, respectively. We discerned that all type I ZnO NW devices are gathering in Region A indicating two Ohmic contacts on the individual ZnO NW. It is noted that the type I devices have RT resistances lower than 100 kΩ. In addition, type II devices distribute in Region B and unveil one-dimensional VRH conduction in one and only one nanocontact on the ZnO NW. Unlike type I and II devices, type III devices, having RT resistances higher than 100 kΩ, spread over Region B and C that connotes two- and three-dimensional VRH conduction in both nanocontacts of a NW device. In Figure 5b, we provide three nanocontact models to elaborate our thoughts. Since a direct Ti metal contacting on ZnO should be attributed to Ohmic contacts as inferred from experiments of bulk systems,[36] we propose a direct contacting model for nanocontacts of ZnO NW devices in Region A. Otherwise, the RT resistance is greater for devices in Regions B and C, we argue that titanium oxide form in the nanocontacts due to poor vacuum conditions during thermal evaporation. For NW devices in Region B, we believe that the oxide layer is thin enough for electrons to transport as one-dimensional VRH conduction. When the oxide layer is thick, the conduction channels mix to form two- and three-dimensional VRH conduction such as the proposed nanocontact model for devices in Region C.

In summary, the shrinkage of contact area multiplies the nanocontact resistance to dominate the overall electrical properties of the two-contact NW nanoelectronic devices. The ZnO NW devices with contact electrodes kept at the

same distance could be categorized into three different types. Type I ZnO NW devices, having RT resistances less than 100 kΩ, reveal an Ohmic-type linear $I-V$ dependence and evidence intrinsic NW electrical properties of thermally activated transport in electron conduction through the ZnO NWs. Type II devices, having RT resistances between 100 kΩ and 10 MΩ, display rectifying $I-V$ behaviors, and they demonstrate one-dimensional VRH conduction in the solely Schottky type nanocontact of the device. For type III devices, the NW devices could be modeled as two back-to-back Schottky contact and their $I-V$ curves conform justly to the mathematical form of thermionic-emission theory. The temperature dependent resistance indicates either one- or high-dimensional VRH conduction in the nanocontacts of the type III ZnO NW devices.

Acknowledgment. The authors thank Prof. Ji-Jung Kai and Prof. Fu-Rong Chen for providing ZnO nanowires and Prof. Juhn-Jong Lin for his instrumentation support. This work was supported by the Taiwan National Science Council under Grant NSC 95-2112-M-009-045-MY3 and by the MOE ATU Program.

References

(1) Iijima, S. *Nature* **1991**, *354*, 56.
(2) Brus, L. *J. Phys. Chem.* **1994**, *98*, 3575.
(3) Morales, A. M.; Lieber, C. M. *Science* **1998**, *279*, 208.
(4) Li, Y.; Meng, G. W.; Zhang, L. D.; Phillipp, F. *Appl. Phys. Lett.* **2000**, *76*, 2011.
(5) Pan, Z. W.; Dai, Z. R.; Wang, Z. L. *Science* **2001**, *291*, 1947.
(6) Vayssieres, L *Int. J. Nanotechnol.* **2004**, *1*, 1.
(7) Lu, W.; Lieber, C. M. *Nat. Mater.* **2007**, *6*, 841.
(8) Tans, S. J.; Verschueren, A. R. M.; Dekker, C. *Nature* **1998**, *393*, 49.
(9) Ebbesen, T. W.; Lezec, H. J.; Hiura, H.; Bennett, J. W.; Ghaemi, H. F.; Thio, T. *Nature* **1996**, *382*, 54.
(10) Wang, X.; Song, J.; Liu, J.; Wang, Z. L. *Science* **2007**, *316*, 102.
(11) Kind, H.; Yan, H.; Messer, B.; Law, M.; Yang, P. *Adv. Mater.* **2002**, *14*, 158.
(12) Wan, Q.; Li, Q. H.; Chen, Y. J.; Wang, T. H.; He, X. L.; Li, J. P.; Lin, C. L. *Appl. Phys. Lett.* **2004**, *84*, 3654.
(13) Fan, Z.; Wang, D.; Chang, P. C.; Tseng, W. Y.; Lu, J. G. *Appl. Phys. Lett.* **2004**, *85*, 5923.
(14) Heo, Y. W.; Tien, L. C.; Kwon, Y.; Norton, D. P.; Pearton, S. J.; Lang, B. S.; Ren, F. *Appl. Phys. Lett.* **2004**, *85*, 2274.
(15) Park, W. I.; Kim, J. S.; Yi, G. C.; Bae, M. H.; Lee, H. J. *Appl. Phys. Lett.* **2004**, *85*, 5052.
(16) Heo, Y. W.; Tien, L. C.; Norton, D. P.; Pearton, S. J.; Kang, B. S.; Ren, F.; LaRoche, J. R. *Appl. Phys. Lett.* **2004**, *85*, 3107.
(17) Lao, C. S.; Liu, J.; Gao, P.; Zhang, L.; Davidovic, D.; Tummala, R.; Wang, Z. L. *Nano Lett.* **2006**, *6*, 263.
(18) Park, W. I.; Kim, J. S.; Yi, G. C.; Lee, H. *J. Adv. Mater.* **2005**, *17*, 1393.
(19) Bao, J.; Zimmler, M. A.; Capasso, F.; Wang, X.; Ren, Z. F. *Nano Lett.* **2006**, *6*, 1719.
(20) Zhang, Z.; Yao, K.; Liu, Y.; Jin, C.; Liang, X.; Chen, Q.; Peng, L. M. *Adv. Funct. Mater.* **2007**, *17*, 2478.
(21) Ma, Y. J.; Zhang, Z.; Zhou, F.; Lu, L.; Jin, A.; Gu, C. *Nanotechnology* **2006**, *16*, 746.
(22) Léonard, F.; Talin, A. A. *Phys. Rev. Lett.* **2006**, *97*, 026804.
(23) Bachtold, A.; Henny, M.; Terrier, C.; Strunk, C.; Schönenberger, C.; Salvetat, J. P.; Bonard, J. M.; Forró, L. *Appl. Phys. Lett.* **1998**, *73*, 274.
(24) Stern, E.; Cheng, G.; Young, M. P.; Reed, M. A. *Appl. Phys. Lett.* **2006**, *88*, 053106.
(25) Lin, Y. F.; Jian, W. B.; Wang, C. P.; Suen, Y. W.; Wu, Z. Y.; Chen, F. R.; Kai, J. J.; Lin, J. J. *Appl. Phys. Lett.* **2007**, *90*, 223117.
(26) Jian, W. B.; Chen, I. J.; Liao, T. C.; Ou, Y. C.; Nien, C. H.; Wu, Z. Y.; Chen, F. R.; Kai, J. J.; Lin, J. J. *J. Nanosci. Nanotechnol.* **2008**, *8*, 202.
(27) Kittel, C. *Introduction to Solid State Physics*; John Wiley & Sons: Edison, New Jersy, 2005; p 147.
(28) Sze, S. M.; Ng, K. K. *Physics of Semiconductor Devices*; John Wiley & Sons: Edison, NY, 2007; p 25.
(29) Rhoderick, E. H.; Williams, R. H. *Metal-Semiconductor Contacts*; Clarendon Press: Oxford, 1988; p 99.
(30) Mott, N. F. *Conduction in Non-Crystalline Materials*; Clarendon Press: Oxford, 1993; p 32.
(31) Wu, Z. Y.; Chen, I. J.; Lin, Y. F.; Chiu, S. P.; Chen, F. R.; Kai, J. J.; Lin, J. J.; Jian, W. B. *New J. Phys.* **2008**, *10*, 033017.
(32) Heo, Y. W.; Tien, L. C.; Norton, D. P.; Kang, B. S.; Ren, F.; Gila, B. P.; Pearton, S. J. *Appl. Phys. Lett.* **2004**, *85*, 2002.
(33) Chang, P. C.; Lu, J. G. *Appl. Phys. Lett.* **2008**, *92*, 212113.
(34) Nam, C. Y.; Tham, D.; Fischer, J. E. *Nano Lett.* **2005**, *5*, 2029.
(35) Hernandez-Ramirez, F.; Tarancon, A.; Casals, O.; Pellicer, E.; Rodriguez, J.; A. Romano-Rodriguez, A.; Morante, J. R.; Barth, S.; Mathur, S. *Phys. Rev. B* **2007**, *76*, 085429.
(36) Ip, K.; Thaler, G. T.; Yang, H.; Han, S. Y.; Li, Y.; Norton, D. P.; Pearton, S. J.; Jang, S.; Ren, F. *J. Cryst. Growth* **2006**, *287*, 149.

NL801347X